Supplementary Information

A multi-responsive intrinsically disordered protein (IDP)-directed green synthesis of fluorescent gold nanoclusters

Rajkamal Balu,[a] Laure Bourgeois,[b] Christopher M. Elvin,[c] Anita J. Hill,[d] Namita R. Choudhury,*[a] and Naba K. Dutta,*[a]

[a] Ian Wark Research Institute, University of South Australia, Mawson Lakes, SA 5095, Australia.

[b] Monash Centre for Electron Microscopy, Department of Materials Engineering, Monash University, Clayton, VIC 3800, Australia.

[c] CSIRO Agriculture, Level 6, Queensland Bioscience Precinct, St Lucia, QLD 4067, Australia.

[d] CSIRO Manufacturing, Clayton, VIC 3168, Australia.

* Correspondence E-mail: naba.dutta@unisa.edu.au; namita.choudhury@unisa.edu.au

S1. Characterization:

S1.1. Molecular weight determination by Matrix Assisted Laser Desorption Ionization Time-of-Flight (MALDI-TOF) mass spectrometry

For molecular weight determination by MALDI-TOF-MS, pure Rec1-resilin or AuNCs-Rec1-resilin nanobioconjugate was dissolved in 30% acetonitrile, 0.1% trifluoroacetic acid (TA30) to make a final protein concentration of 3 mg ml^{-1}. 1.5 µl of matrix (sinapinic acid, saturated in ethanol) was spotted onto a polished steel target plate (Bruker Daltonics, Bremen, Germany) and air dried. 2 µl of protein solution (1 pmol/µl) was mixed with 2 µl of matrix (sinapinic acid, saturated in TA30). 0.5 µl of the sample-matrix mix was spotted onto the previously created matrix spots and air dried. The measurement range used was m/z 5,000-50,000. 5,000 shots were collected for the external calibration and 20,000 shots for sample measurement. External calibration was performed using a mix of protein calibration standard I and II (Bruker Daltonics). Laser intensity and detector gain were manually adjusted for optimal resolution. The mass spectra obtained were analyzed using flexAnalysis software (version 3.3, Bruker Daltonics) employing smoothing, background subtraction and peak detection algorithms.

S1.2. Transmission electron microscopy (TEM)

TEM was performed on some of the samples in order to characterize their size and crystal structure. The TEM samples were made by simply placing a drop of solution onto a Cu grid coated with an ultra-thin carbon film. TEM and scanning (S)-TEM were performed on a dual aberration corrected FEI Titan^3 80-300 at an accelerating voltage of 300 kV. In TEM mode the image corrector was tuned to a spherical aberration value of Cs = +1μm, resulting in an image resolution of better than 1 Å. Images were collected on a Gatan Ultrascan CCD with an exposure time of 0.5 s. The Fast Fourier Transforms were performed using ImageJ software. STEM was carried out with a convergence semi-angle of 15 mrad, yielding a probe size of ~1 Å and hence the best achievable resolution in this condition of ~1 Å. The STEM images were collected in high-angle annular dark field (HAADF) mode with an inner collection semi-angle of 55 mrad. No image processing was performed on the STEM data other than minor adjustments in brightness and contrast.

High-resolution TEM image simulations were carried out on JEMS software for the face-centred cubic (FCC) crystal structure of Au (a = 0.408 nm) in order to establish the nature of the correspondence between structure and image.[1] As shown in Fig. S9 for the viewing direction of [110], a Au crystal less than 6 nm in thickness imaged with a defocus of less than 12 nm (area framed in red) will exhibit strong black contrast at the positions of atomic columns (yellow dots overlapped over bottom left image). Both these thickness and defocus conditions were met in the present experiments, since the nanoparticles were always less than 3 nm, and overwhelmingly less than 2 nm in diameter. Furthermore the defocus of the objective lens was carefully controlled to be less than 10 nm. Therefore, the dark contrasts observed in HRTEM images such as shown in Fig. 6 of the main document can be interpreted as atomic columns.

S1.3. HOMO-LUMO gap determination

The HOMO-LUMO gap of blue and green fluorescent AuNCs has been evaluated from the absorption spectrum using the Tauc relation:[2]

$$\alpha h\nu = C(h\nu - E_g)^{1/2} \quad \ldots(1)$$

where C is a constant, α is the absorption coefficient, E_g is the average energy gap of the material. The average optical band gap was estimated from the intercept of linear portion of the $(\varepsilon h\nu)^2$ vs. hν plots on hν axis as shown in Fig. S7.

Figures:

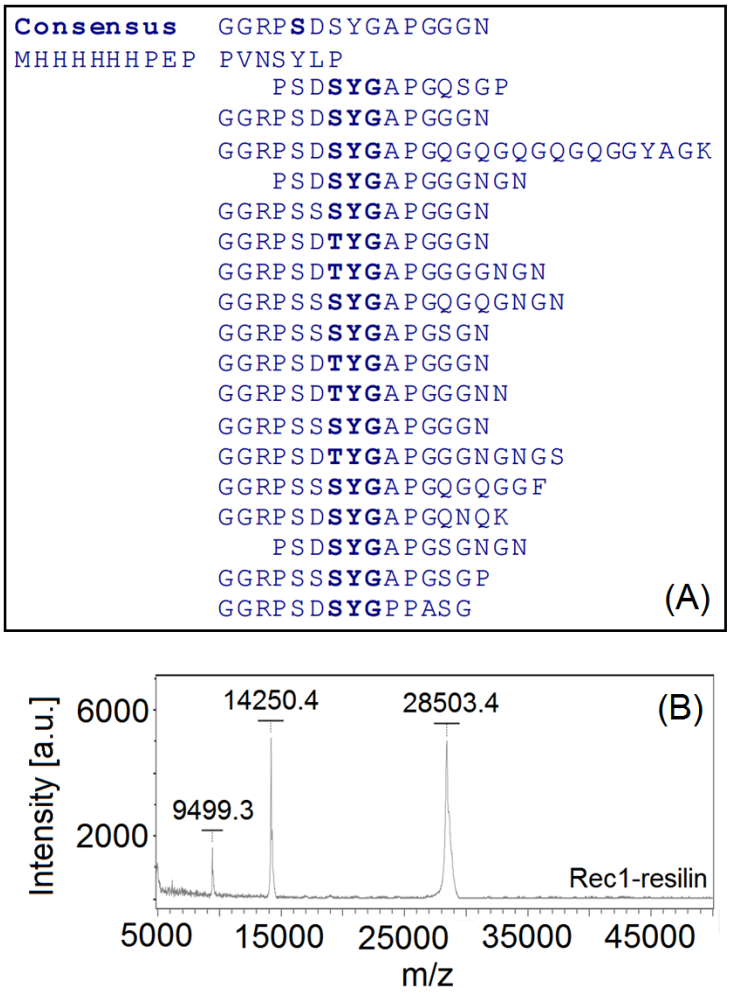

Fig. S1. (A) Structural consensus and alignment of amino acid repeat sequence in Rec1-resilin. Single-letter code is used. (B) MALDI-TOF mass spectra of synthesized Rec1-resilin. The three m/z species (right to left) detected are the $[M+H]^{+}$, $[M+2H]^{2+}$, and $[M+4H]^{4+}$ species of the protein.

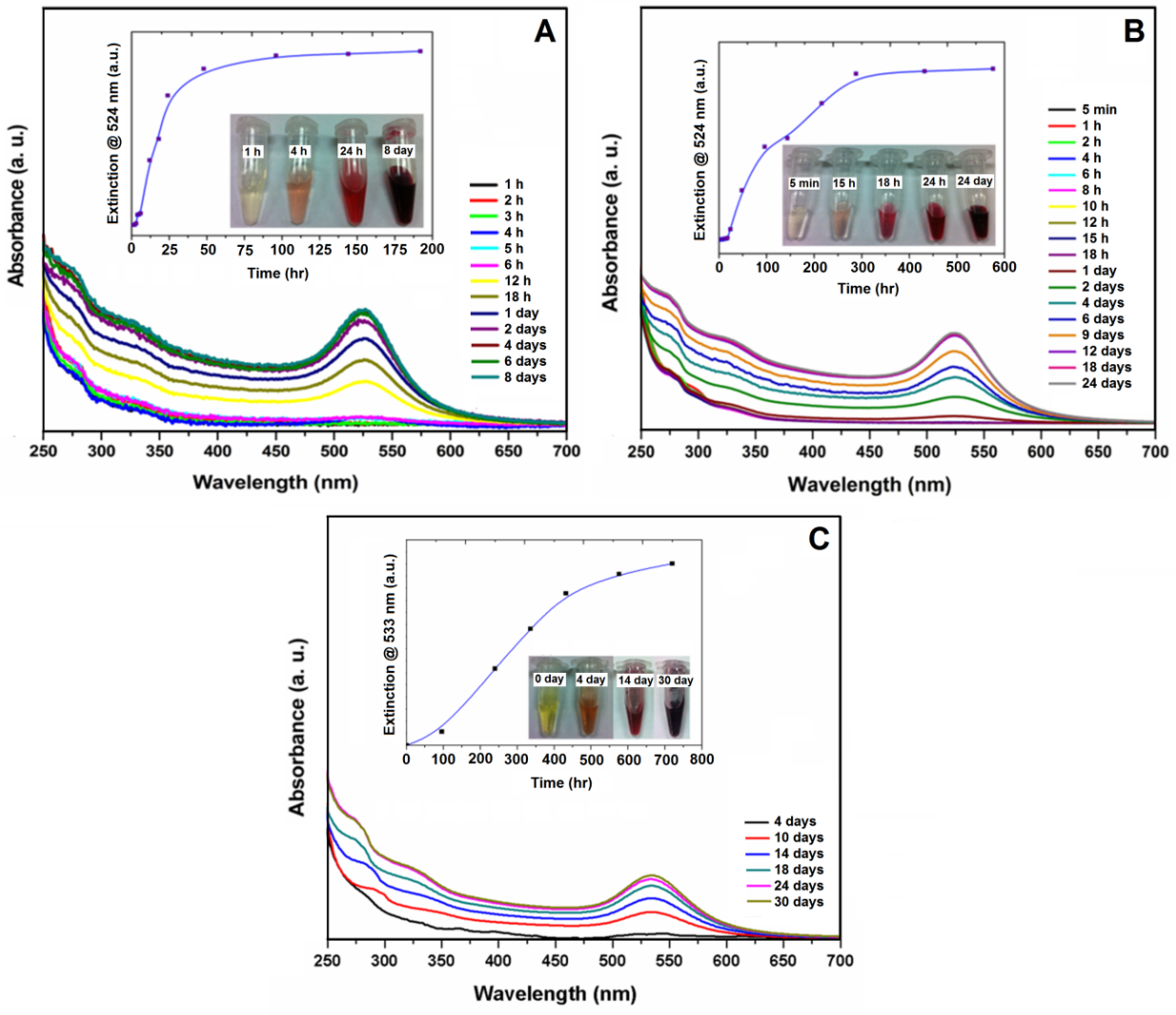

Fig. S2. UV-Vis spectrum of chloroauric acid reduction kinetics by Rec1-resilin (Au:protein molar ratio of 16) over time at (a) 70 °C, (b) 50 °C, and (c) 37 °C. Insets: corresponding evolution of the absorbance peak intensity at λ_{max} (524 nm for 70 °C and 50°C; 533 nm for 37 °C) as a function of time.

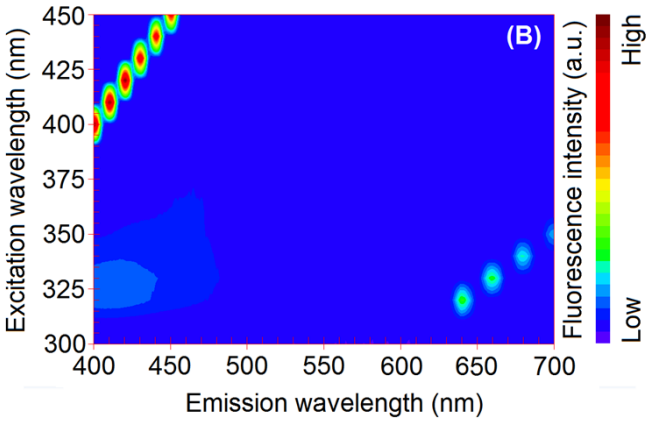

Fig. S3. 3D excitation-emission contour plot of Rec1-resilin equilibrated at 50 °C for 10 days.

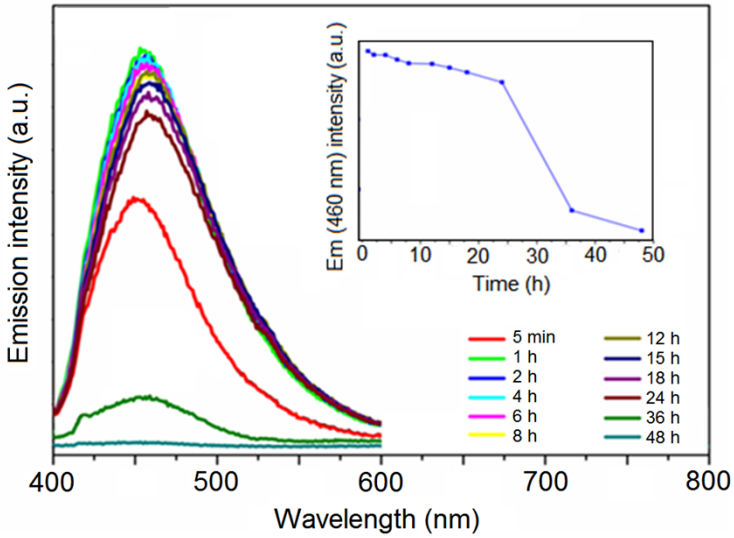

Fig. S4. Plot showing the progressive extinction of Au^0 nuclei fluorescence over reaction time at 50 °C (excitation wavelength of 380 nm). The inset of the plot shows the fluorescence decay with time.

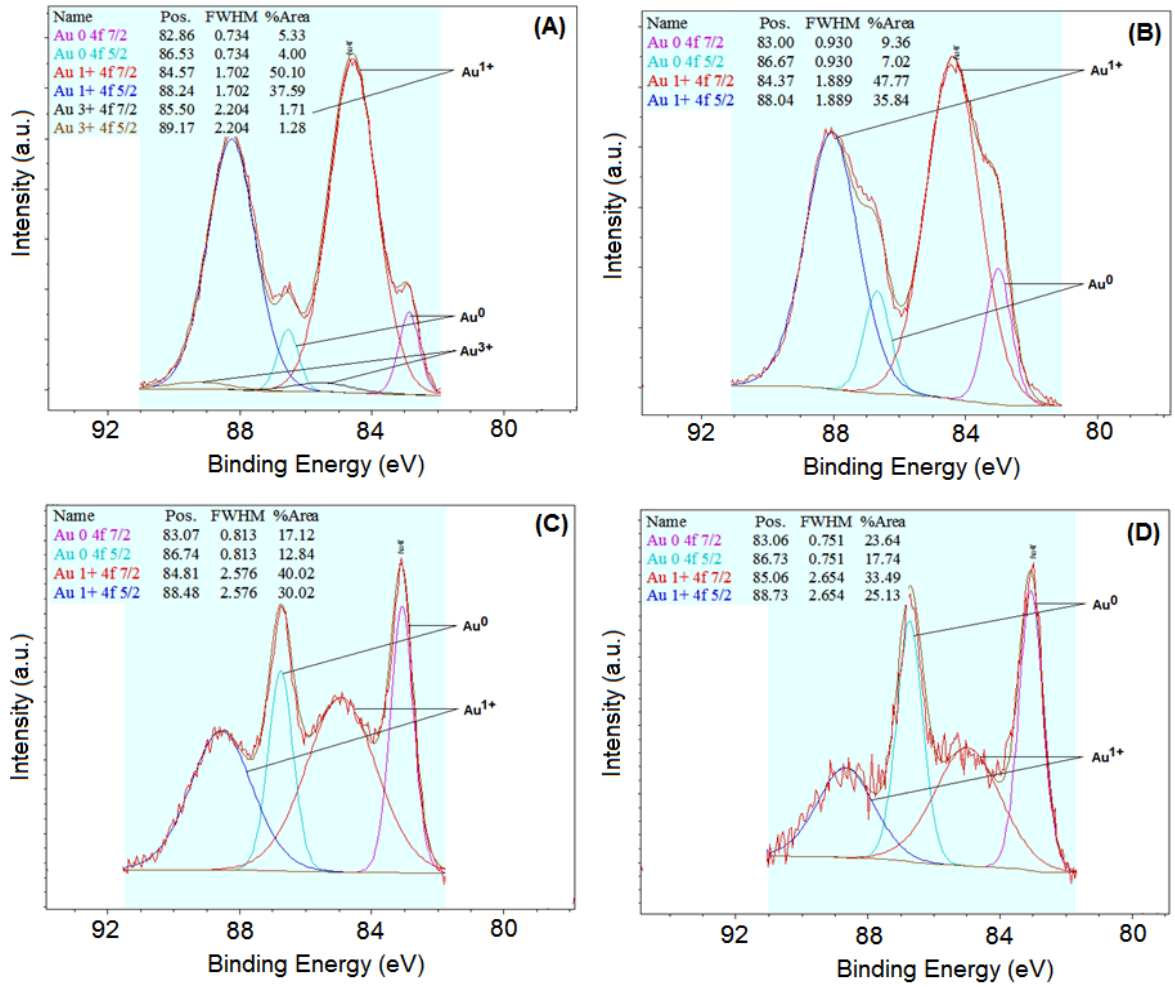

Fig. S5. XPS spectra of Au chemical state in Au: protein molar ratio of 16 samples over time (a) 5 min, (b) 1 h, (c) 9 days, and (d) 24 days at 50 °C.

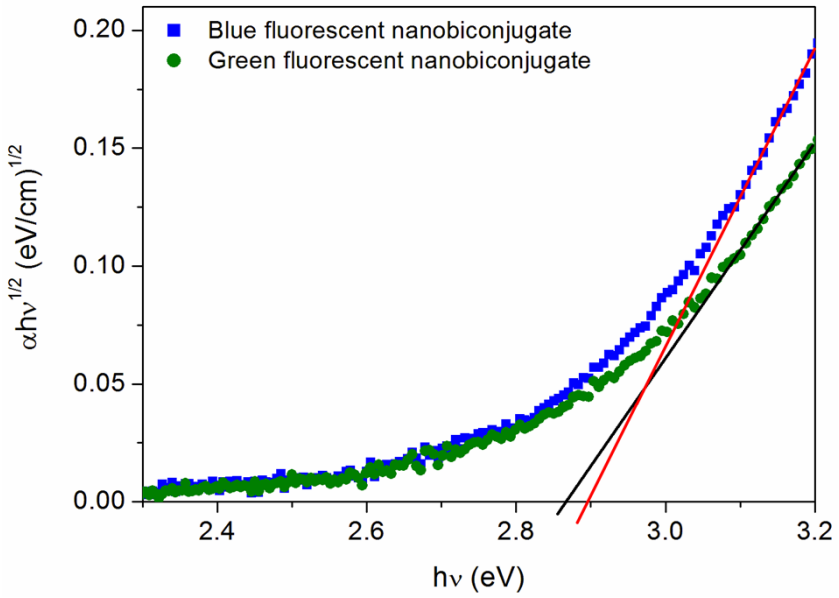

Fig. S6. Tauc plot for HOMO-LUMO gap determination of blue and green fluorescent AuNCs.

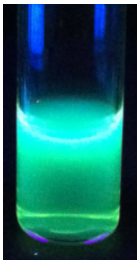

Fig. S7. Photograph of green fluorescent AuNCs-Rec1-resilin nanobioconjugate under 365 nm UV light after incubation at room temperature (~23 °C) for almost a year.

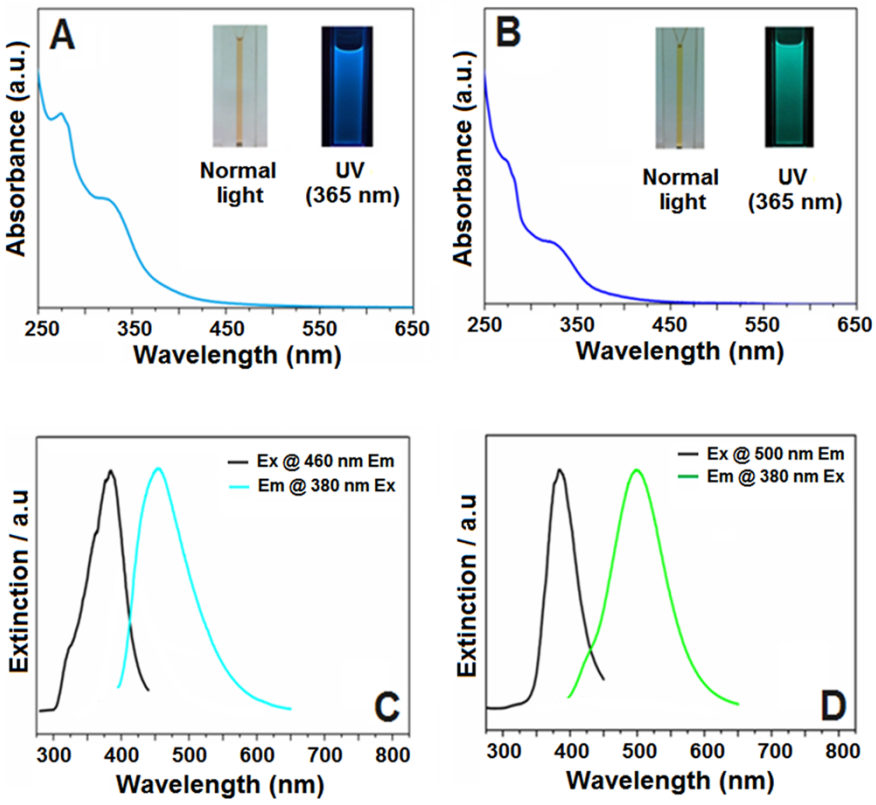

Fig. S8. UV-Vis absorption spectra of (A) blue and (B) green fluorescent AuNCs-Rec1-resilin nanobioconjugate. Excitation and fluorescence emission spectra of (C) blue and (D) green fluorescent AuNCs-Rec1-resilin nanobioconjugate.

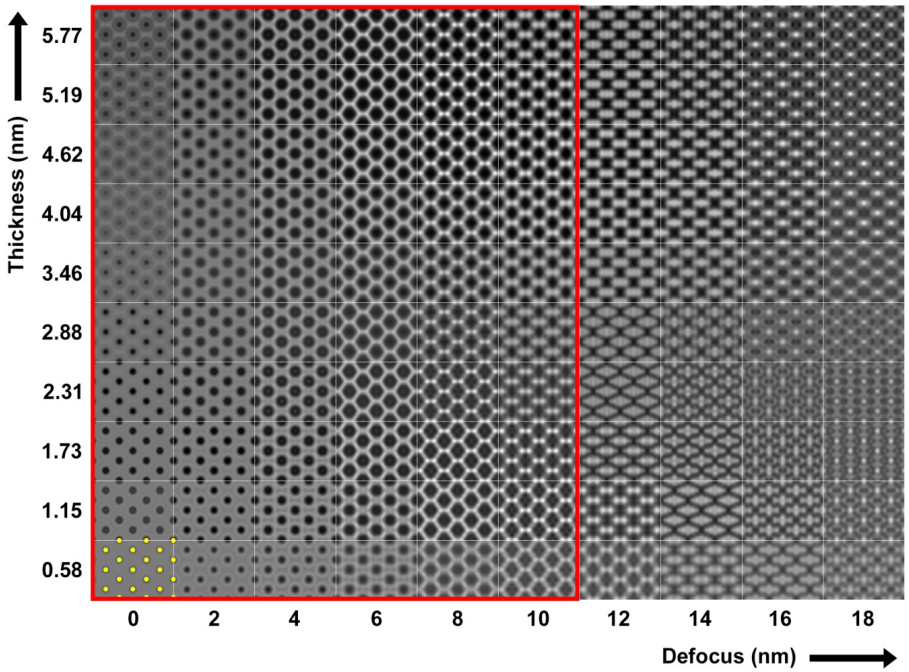

Fig. S9. HRTEM image simulations of the FCC structure of Au viewed along [110], as a function of thickness and defocus.

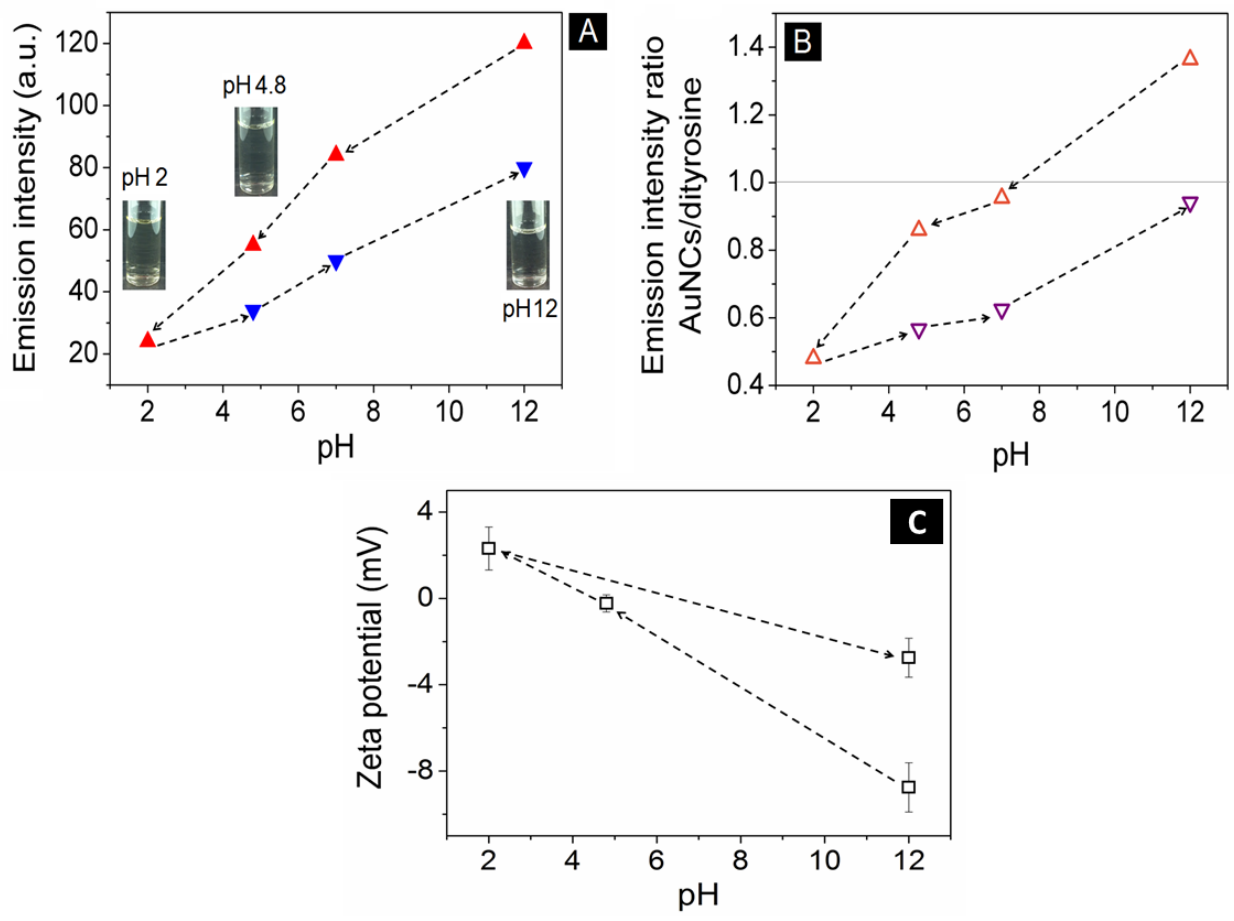

Fig. S10. (A) The plot of fluorescence intensity of green fluorescent AuNCs-Rec1-resilin nanobioconjugate as a function of pH in forward (pH 12 to 2) and reverse (pH 2 to 12) cycles. Insets: corresponding optical pictures of nanobioconjugate solution. The intensity of AuNCs and protein's dityrosine in reverse cycle was measured to be less than that measured at respective pH in forward cycling, which may be related to the dilution (B) Emission intensity ratio (AuNCs to dityrosine) of green fluorescent AuNCs-Rec1-resilin nanobioconjugate. (C) The plot of zeta potential of green fluorescent AuNCs-Rec1-resilin nanobioconjugate as a function of pH in forward (pH 12 to 2) and reverse (pH 2 to 12) cycles.

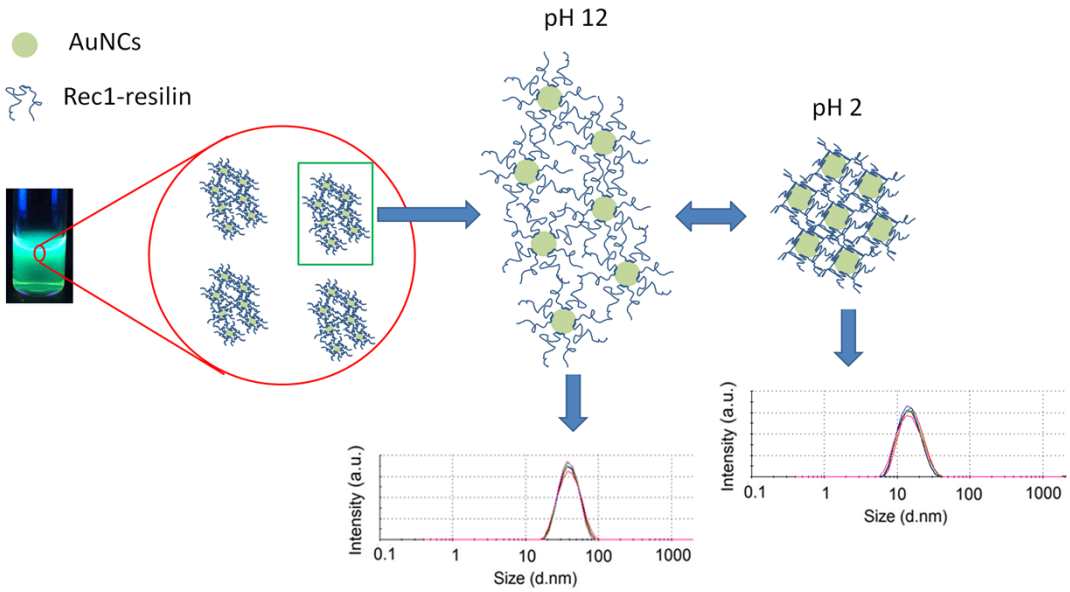

Fig. S11. Proposed schematic of the AuNCs-Rec1-resilin nanobioconjugate at pH ~12 and ~2.

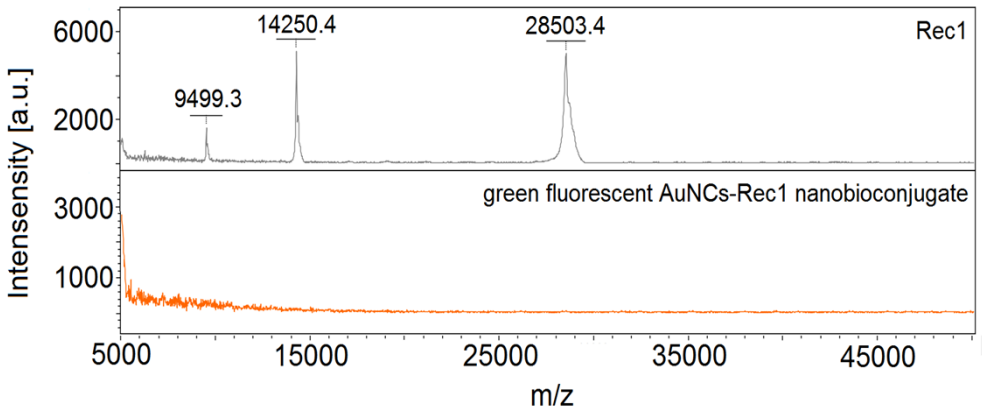

Fig. S12. MALDI-TOF mass spectra of green fluorescent AuNCs-Rec1-resilin nano-bioconjugate. MALDI-TOF mass spectrum of Rec1-resilin is presented as a reference, where the three characteristic m/z species (right to left); $[M+H]^+$, $[M+2H]^{2+}$, and $[M+4H]^{4+}$ are clearly identified.

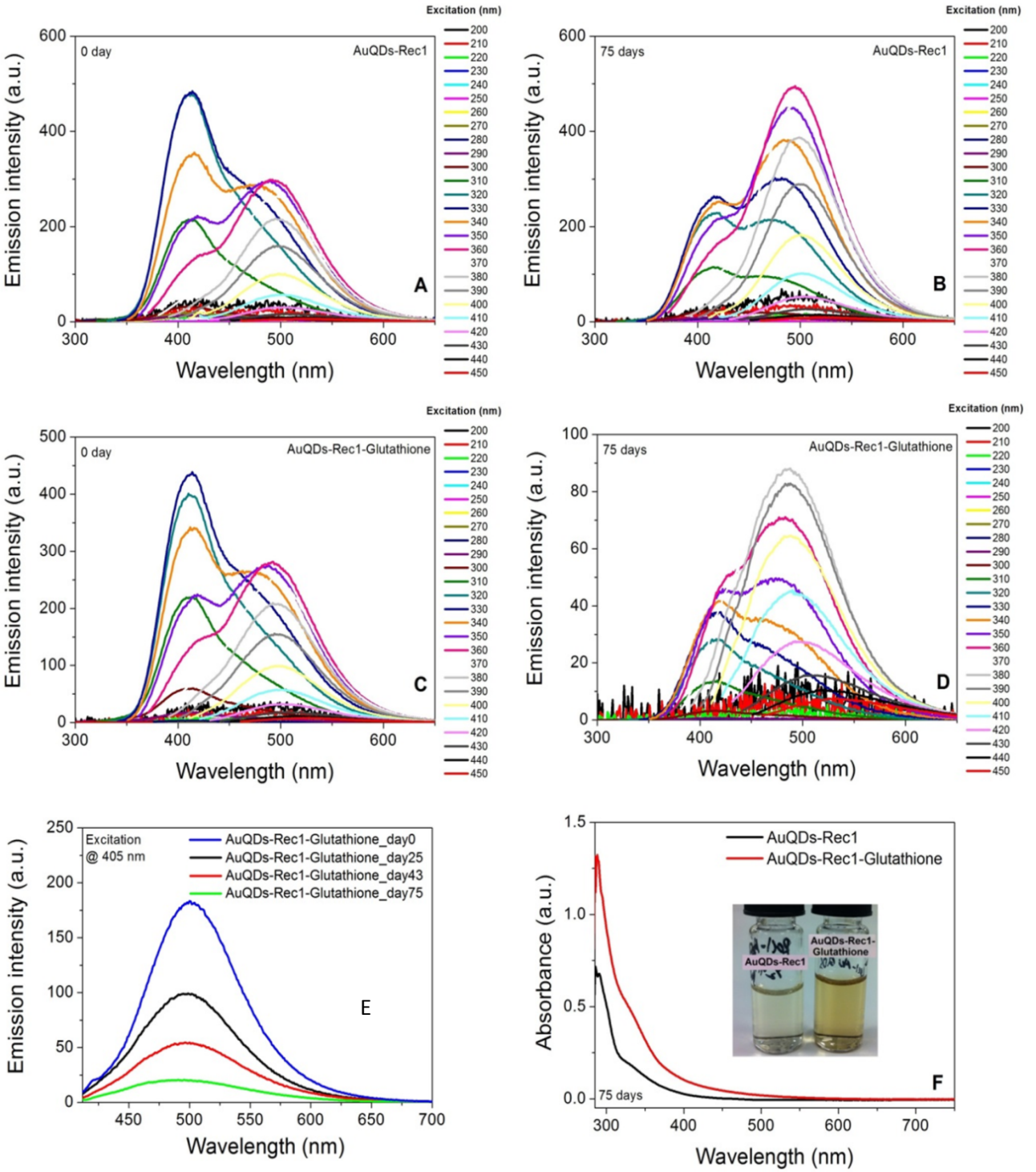

Fig. S13. Fluorescence spectrum of (A) Freshly prepared green fluorescent AuNCs-Rec1-resilin nano-bioconjugate (Au:protein molar ratio 2); (B) After ageing for 75 days; (C) After addition of glutathione to freshly prepared AuNCs-Rec1-resilin nano-bioconjugate; (D) AuNCs-Rec1-resilin nano-bioconjugate after addition of glutathione to freshly prepared green fluorescent AuNCs-Rec1-resilin nano-bioconjugate; (E) Evolution of the fluorescence spectrum of AuNCs-Rec1-resilin nano-bioconjugates with time after addition of glutathione; (F)

UV/Vis-Spectrum of green fluorescent AuNCs-Rec1-resilin nano-bioconjugate with and without glutathione after ageing for 75 days.

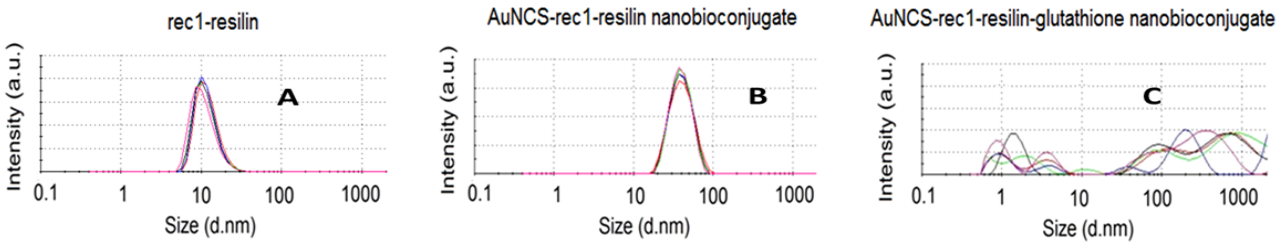

Fig. S14. Hydrodynamic diameter of (A) Rec1-resilin (B) AuNCs-Rec1-resilin nano-bioconjugate. (C) Effect of addition of glutathione on hydrodynamic diameter of AuNCs-Rec1-resilin nanobioconjugate.

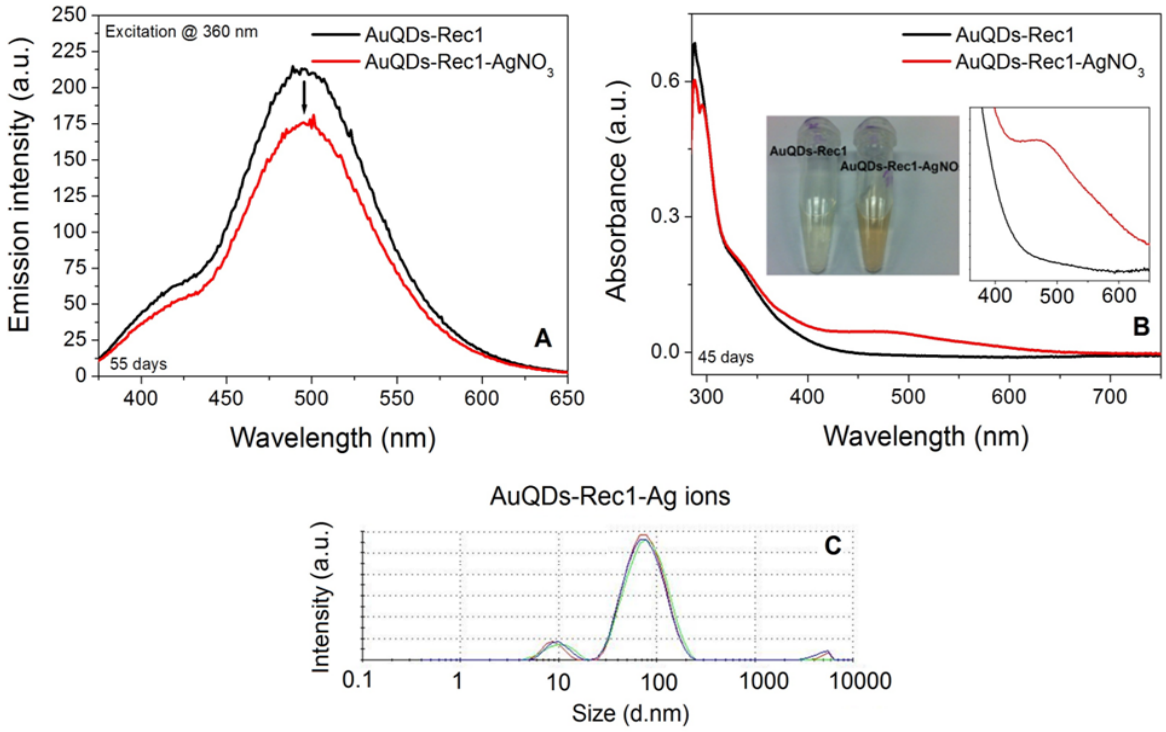

Fig. S15. Effect of addition of $AgNO_3$ on the properties of green fluorescent AuNCs-Rec1-resilin nano-bioconjugate. (A) Influence on fluorescence with Ag ions upon ageing for 55 days; (B) Effect of the Ag ions on the UV-Vis spectrum upon ageing for 45 days; (C) Effect of addition of Ag ions on hydrodynamic diameter of AuNCs-Rec1-resilin nanobioconjugate.

References

1. P. Stadelmann, EMS Java Version 3, CIME-EPFL: Lausanne, Switzerland, 1999.
2. J. Tauc and A. Menth, *J. Non-Cryst. Solids*, 1972, **8**, 569-585.